

Temporal Changes of Soil Surface Conditions Related to Wind Erosion

Roger Funk and Monika Frielinghaus

1. Introduction

The erodibility of sandy soils is substantially influenced by the actual soil surface conditions. Texture, organic matter content, water content and exterior factors like precipitation or soil management have to be taken into consideration in their manifold combinations in time and space. The surface properties can change within short times and with local differences. Therefore, predictions of the actual erosion risk are difficult and often inaccurate. A need can be derived for the accurate description of the dynamic of the soil surfaces properties to prevent wind erosion as well as environmental pollution or damages to young plants.

Sandy soils generally are considered to be high erodible. Erodibility can be reduced or prevented by external factors like precipitation, which initiate cohesive forces by moisture or surface crusts. Besides precipitation smoothing the surface, it increases the near surface bulk density (ZOBECK AND CAMPBELL 1990) and leads to the vertical sorting of the fractions on the surface (VALENTIN AND BRESSON 1992). These sorting processes produce loose erodible material (LEM), which is defined as loose, unconsolidated soil material with a diameter less than 0.84 mm (CHEPIL 1951). The LEM is the initial material to destroy the formed crusts by abrasion. After drying of the soil surface, further erosion depends on the amount of LEM, the crust stability and the crust thickness.

Sandy soils show great differences in their erosion rates, even if they are in the same textural class. The estimation of erodibility for the three “main” fractions (sand, silt and clay) and the organic matter content appears too rough for the sensitive wind erosion process. The sand class contains erodible (< 0.8 mm) and nonerodible (> 0.8 mm) particles which have to be distinguished. Especially the most erodible fractions, medium and fine sand have to be taken into more detailed consideration. Therefore, the selection of soils for investigation was orientated on differences in the sand subclasses rather than on clear textural differences.

2. Materials and Methods

The erodibility of 10 sandy soils was investigated under the aspect of short time changes. Selected parameters to describe these changes were:

1. Loose erodible material (LEM),
2. crust strength,
3. crust stability and
4. soil surface moisture.

Soil samples from the plough horizon (5 – 25 cm) were taken from 9 locations with frequent wind erosion. Additional samples of dune sand and loess, which represent the highest and lowest erodibility in this selection, were integrated into the investigation. The results of the texture analyses are given in Table 1.

Table 1: Particle size distribution for the investigated soils *

Shorthand Expression	Textural Class	Total Sand	CS >630 μm	MS >200 μm	FS >100 μm	VFS >63 μm	Silt 63-2 μm	Clay <2 μm	Humus (%)
Mue	LS	82.53	5.37	39.83	29.40	7.93	14.04	3.43	0.68
Got	LS	87.34	3.97	29.53	41.17	12.67	10.93	1.73	1.33
Kuh	S	91.83	1.60	45.80	36.86	7.57	6.94	1.23	2.42
Lue	S	87.80	0.43	7.47	59.87	20.03	9.40	2.80	1.89
Grk	SL	72.84	3.50	24.07	31.57	13.70	24.73	2.43	1.28
Red	S	90.10	0.75	23.40	57.53	8.42	8.36	1.53	1.93
Bae	SL	72.03	4.73	31.97	26.53	8.80	20.10	7.87	1.67
Loess	SiL	25.26	1.70	11.53	8.20	3.83	64.94	9.80	1.57
Rhi	**	74.38	4.77	26.67	30.87	12.07	14.94	10.70	23.3
Hei	**	83.24	6.80	36.37	34.40	5.67	9.97	6.80	24.6
Dune	S	99.10	0.70	15.30	79.90	3.30	0.30	0.0	0.0

* Codes according to FAO (1990)

** Organic soils

General

The investigations were made in containers with a size of 60 x 30 x 20 cm (length, width, depth). The containers have inlets for tensiometers in 3, 6 and 12 cm depth and a bottom with a permeable foil to simulate the soil suction (Figure 1). The soils were filled into the containers and compacted to their natural bulk density (between 1.45 – 1.65 g/cm³). Rainfall was applied with kinetic energy of 550, 1100 and 1650 J/m² (20, 40 and 60 mm) by a constant intensity of 20 mm/h. During the rainfall simulation the surplus water was sucked off by a vacuum system with 80 – 120 hPa (according to the field capacity of sandy soils). Each rainfall event started the following cycle:

1. Filling and compaction of the soils into the containers (bare, smooth surface)
2. Rainfall simulation
3. Drying (at the same time measuring of the soil water content at the surface and in 3, 6 and 12 cm depth, see also figure 1)
4. Collection of the loose erodible material with a modified vacuum cleaner
5. Crust strength measurement with a penetrometer.

A wind tunnel was used to estimate the stability of aggregates. Crust stability was derived from results of abrading artificial aggregates.

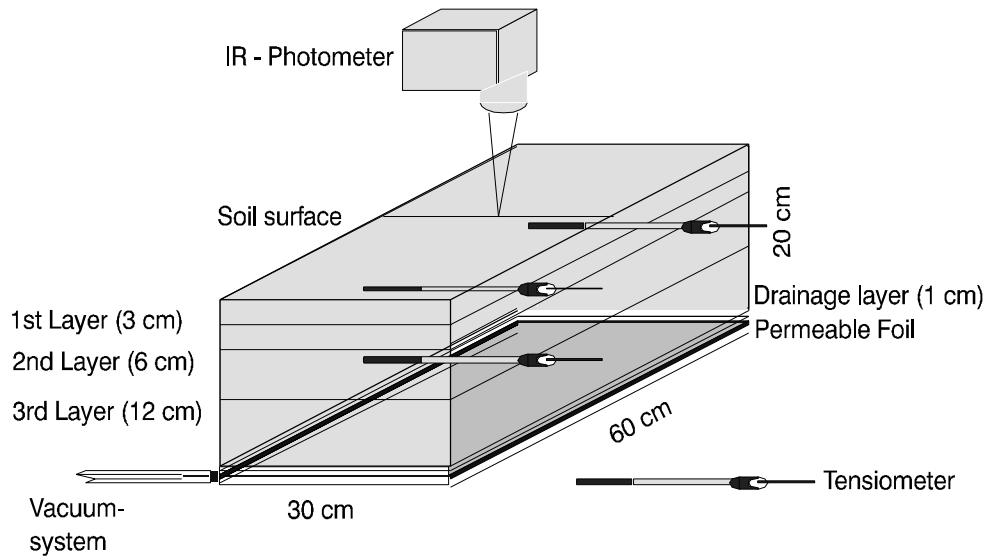


Figure 1: Technical design of the measuring containers and the evaporation measurements

Surface Drying

The investigations of surface drying started if the soil water content reached the field capacity. Surface water content in mass percent [g/100g] and the suction of the tensiometers [kPa] were recorded in a data logger. The experiments were carried out in a laboratory to guarantee controlled conditions. Wind of about 2 m s^{-1} was blown over the surfaces to speed up the evaporation.

Because the natural climatic conditions after rainfall (or saturation of the soil surface) are different in every case, the surface drying should be described rather by climatic quantities with influence on evaporation than only by time (REGINATO 1975, IDSO et al. 1975). The driving force of the surface drying is the vapor pressure deficit of the air. The potential evaporation (E_p) was calculated hourly from wind velocity, air temperature and relative humidity with a modified Penman-Equation of WENDLING (1991):

$$E_p = g \cdot \left(\frac{G}{410} + (0.5 + 0.54 \cdot u) \cdot \left(\frac{100 - RH}{905} \right) \right) \quad [\text{mm h}^{-1}]$$

With $g = 2.4 \cdot \left(\frac{t + 22}{t + 123} \right)$

t	air temperature	[°C]
u	wind velocity	[m s ⁻¹]
RH	relative humidity	[%]
G	solar radiation (set to zero in this case, laboratory experiments)	

The potential evaporation in the laboratory was calculated as 0.67 mmh^{-1} . The vapor pressure deficit of the air is related to the water supply ability of the soil. This can be calculated by an equation, which describes the changes of quantity (ΔQ) within a given depth (Δz). The change of soil water content was calculated as the product of a volume (area times thickness of a layer, $A \Delta z$) and the concentration difference (Δc) between layers for a specific time step (Δt) (RICHTER 1986):

$$\Delta Q = \frac{A \cdot \Delta z \cdot \Delta c}{\Delta t}$$

If the water content on the surface came close to zero the experiments were terminated and the soil was removed layer by layer. Therefore a final profile of the soil water content was measured with the IR-Reflexionphotometer. These values were compared with the tension of the same depth at the same time.

Loose Erodible Material (LEM)

The LEM was collected with a vacuum cleaner system after drying the soil surface. The particle size distribution (PSD) of the collected material was estimated and compared with the PSD of the soil. Empirical equations of ZOBECK and POPHAM (1992) were used to calculate the maximum LEM. The influence of soil properties and rainfall intensity on the formation of LEM were described with regression equations.

Crust stability

Crust stability was measured as cone resistance of a penetrometer in the dry soil surface. The cone had an angle of 30 degrees and a length of 30 mm. It was driven by a motor with a penetration rate of 0.2 mm/s. This was slow enough to exclude inertial and viscoelastic effects. The penetration depth was 30 mm. Data of depth and penetration forces were stored in a data logger every second.

The cone resistance can be divided into the friction (along the surface of the cone) and the compression (perpendicular to the surface of the cone) (Figure 2). The cone resistance can be calculated with the following equations (PUNZEL 1993):

Compression	$F_n = 2 \pi * I(r_0, t)$
Friction	$F_t = \mu_{mb} * 2\pi * \text{ctg}(\alpha/2) * I(r_0, t)$
Overall force	$F_c(t) = 2 \pi * (1 + \mu_{mb} * \text{ctg}(\alpha/2)) * I(r_0, t)$
With	$I(r_0, t) = \int_0^{r_0} (r * p(r, t) dr)$
	$p(r, t) = p_0 + k * r + r * a_0 \exp(-\beta * t)$
	r radius
	p ₀ static soil pressure
	k permanent deformation coefficient
	μ_{mb} glide friction coefficient metal – soil
	β subsidence constant

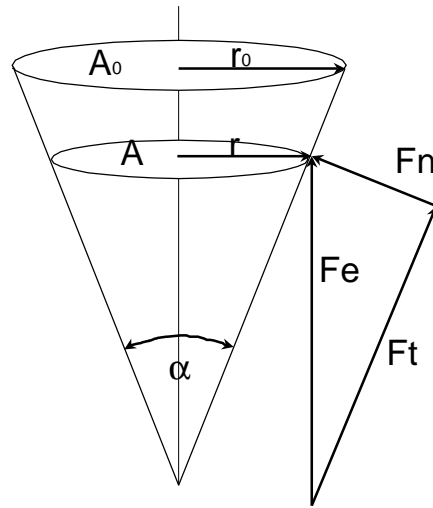


Figure 2: Forces on a cone by penetration

The crust stability was derived from the radial acting normal force of the cone (compression) and related to the cross section area of the cone in this depth. The shear stress of the wind was calculated with $\tau = \rho u_*^2$ and measured on a drag plate in wind tunnel tests. The wind forces were compared with the measured values of the normal force as index of crust stabilities.

Measurements of the friction between cone and soil result in very small forces in loose soil material compared with the cohesive forces of crusted surfaces and were therefore negated.

Aggregate stability

Artificial aggregates were abraded in wind tunnel tests (Fig. 3). Soils were filled in 250 cm³ cylinders, wetted, compacted and air-dried after which the cylinders were removed. The aggregates were exposed an abrasion of sand with a diameter of 0.2 – 0.1 mm and a feeding rate of about 1 gram per second. The abrasion tests were carried out with wind speeds of 8, 10 and 16 m/s. For each run the decrease of mass and volume of the aggregates were measured. Assuming the wind speed is equal to the particle speed, the energy of the abrading particles can be estimated, using the basic equations for kinetic energy or momentum ($W = \frac{1}{2} m v^2$ or $p = mv$). These kinetic forces are faced with the inertial and cohesive forces of the aggregates.

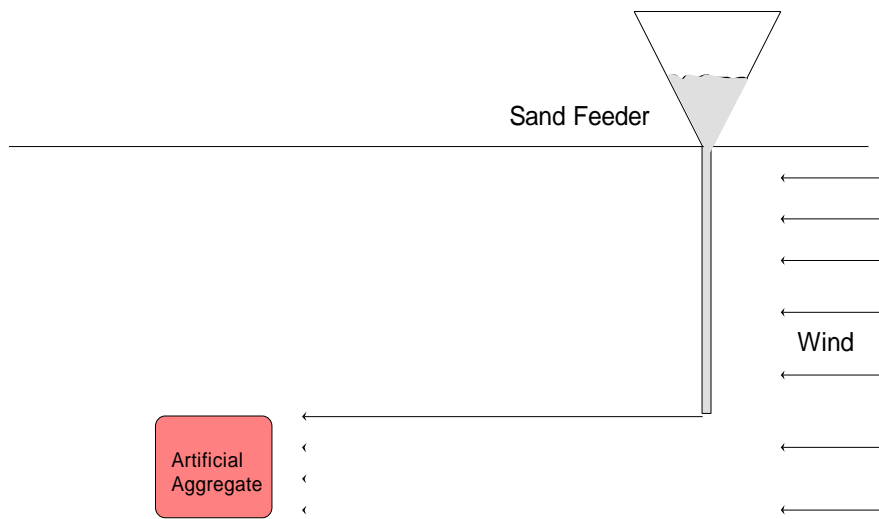


Figure 3: Technical design of the abrasion experiments of artificial aggregates

Results and discussion

Loose Erodible Material (LEM)

The results were obtained on dry soils and therefore, they are only valid for these starting conditions. Generally, the formation of LEM is based on the same principles as the problem of sealing and crusting. The raindrop impacts increased the surface bulk density and decreased the infiltration rate by a vertical size-sorting (VALENTIN 1992). The formation of LEM depends on the ability of the soil to passage the water to the depth. In the case of persistent rainfall LEM is formed until the infiltration rate is fallen short of the precipitation. That point depends on the hydraulic features of the soil. The results show that LEM increases from the first to the second rainfall intensity (550 and 1100 Jm⁻²) and decreases after the third rainfall intensity (1650 Jm⁻²). The change is between 40 mm and 60 mm where the compaction of the surface prevents further undisturbed infiltration. From that point the surplus water on the flat surface in combination with the impact of the raindrops causes a suspension of the surface layer. The clay and silt fractions are dispersed and after drying a depositional crust is formed where the finer particles are above and around the coarser ones.

These results are different from an equation of ZOBECK AND POPHAM (1992) which estimates the decrease of LEM after rain > 10 mm. This difference could be caused by the limitation on sandy soils in this study, as these soils have a good infiltration in general.

The amount of LEM collected after every rainfall simulation was compared with the textural classes of the soils and the kinetic energy of the rainfall. The most LEM was measured after rainfall of 40 mm (1100 Jm⁻²). The basis was the maximum amount of LEM independent of the rainfall amount. In table 2 the results of regression analyzes are listed. The best relation exists to the silt content, a parameter that is also important for crust formation (ROTH 1992).

Table 2: Regression equations between soil parameters and the formation of LEM (g/m²)

Dependent Variable	Independent Variable	A	B	r ²
Log LEM (g/m ²)	Sand (%)	-1.69	0.067	0.46**
	Log Silt (%)	9.51	-2.3	0.62***
	Log Clay (%)	5.22	-2.15	0.52**
	Humus (%)	0.34	1.87	0.33*

The comparison of the grain size distribution between the LEM and the soils show an increase of the fractions 2 – 0.2 mm and a decrease of the fractions smaller than 0.06 mm (Table3, Figure 4). This emphasized the sorting process on the surface.

Table 3: Comparison between the particle size distributions (%) of the soil and the LEM

Soil		>0.6mm	>0.2mm	>0.1mm	>0.06mm	<0.06mm
Mue	LEM	16.8	43.1	29.5	10.5	0
	Soil	5.4	39.8	29.4	7.9	17.5
Got	LEM	8.5	39.9	40.1	10.1	1.4
	Soil	3.9	29.5	41.2	12.6	12.7
Kuh	LEM	4.3	54.7	33.5	6.1	1.2
	Soil	1.6	45.8	36.8	7.6	8.2
Red	LEM	4.7	28.3	51.6	13.4	2.0
	Soil	0.7	23.4	57.5	8.4	9.9
Lue	LEM	4.4	22.5	51.4	19.5	2.2
	Soil	0.43	7.5	59.9	20.0	12.2
Grk	LEM	24.0	40.0	28.0	8.0	0
	Soil	3.5	24.1	31.6	13.7	27.2

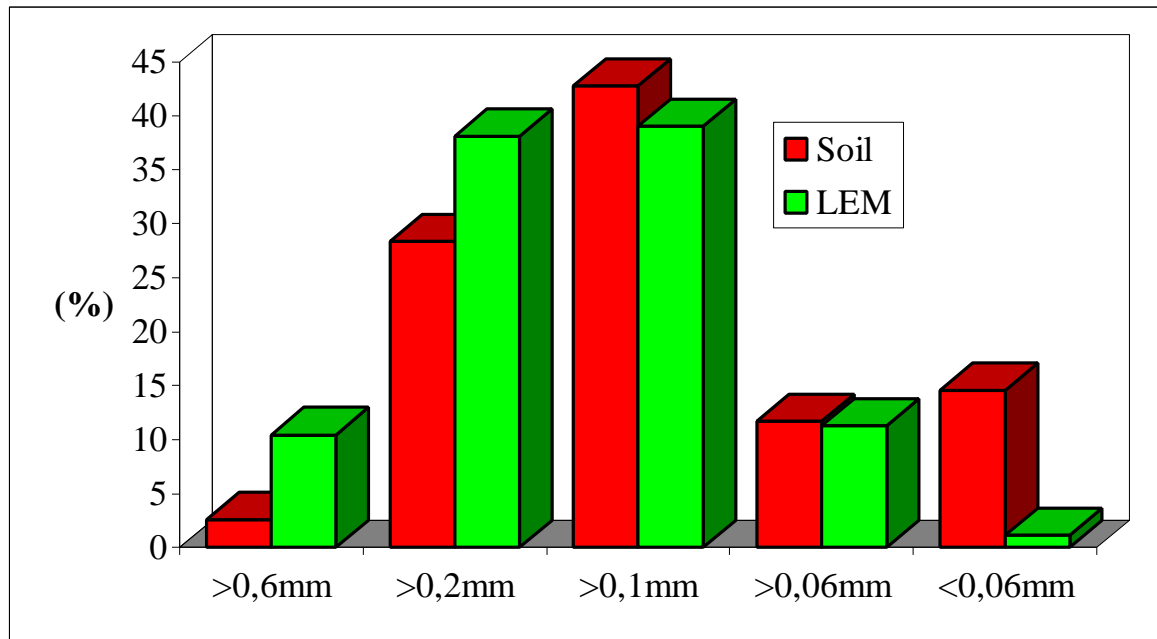


Figure 4: Comparison between the grain size distribution (%) of the soil and the LEM (average of all sandy soils)

A complex consideration of soil and rainfall parameters on the formation of LEM (g/m²) leads to the following equation:

$$\text{Log LEM} = 4.78 + 0.002 E_{\text{kin}} - 0.08 U \quad r^2 = 0.52^*$$

where E_{kin} kinetic energy of the rainfall (J/m²)
 U silt content (kg/kg)

There was no significance to the other fractions.

If there are loose erodible particles on the surface a question will be: What is the amount of the most erodible fraction (medium and fine sand (MS+FS), 125 – 630 μm) and will the increase of this sorted material decrease the threshold conditions for erosion? The results show an increase of these fractions in the LEM related to the original soil but the total amount decreases (Fig. 4 and Fig. 5). A calculation of a theoretical 100% cover with LEM in a layer of 0.2 mm thickness results in an amount of 1250 g/m². From this point of view the relative erodibility will be always reduced compared to the uncrusted soil because the LEM of these fractions reached about a sixth of the soil. But the focus of the MS+FS fractions improves the calculation of the LEM, because both amount to more than 80 % of the total LEM. The relation of LEM (g/m²) can be calculated from the content of MS+FS and the kinetic energy of the rainfall as follows:

$$\text{LEM} = 24.2 + 0.4 (\text{MS+FS})_{\text{Soil}} + 0.04 E_{\text{kin}} \quad r^2 = 0.8^{***}$$

An other way to estimate the LEM is the percentage cover of the surface. This can be done by observation or with simple image processing systems if there are clear colour differences. The percentage cover can be calculated by setting 1250 g/m² for 100%.

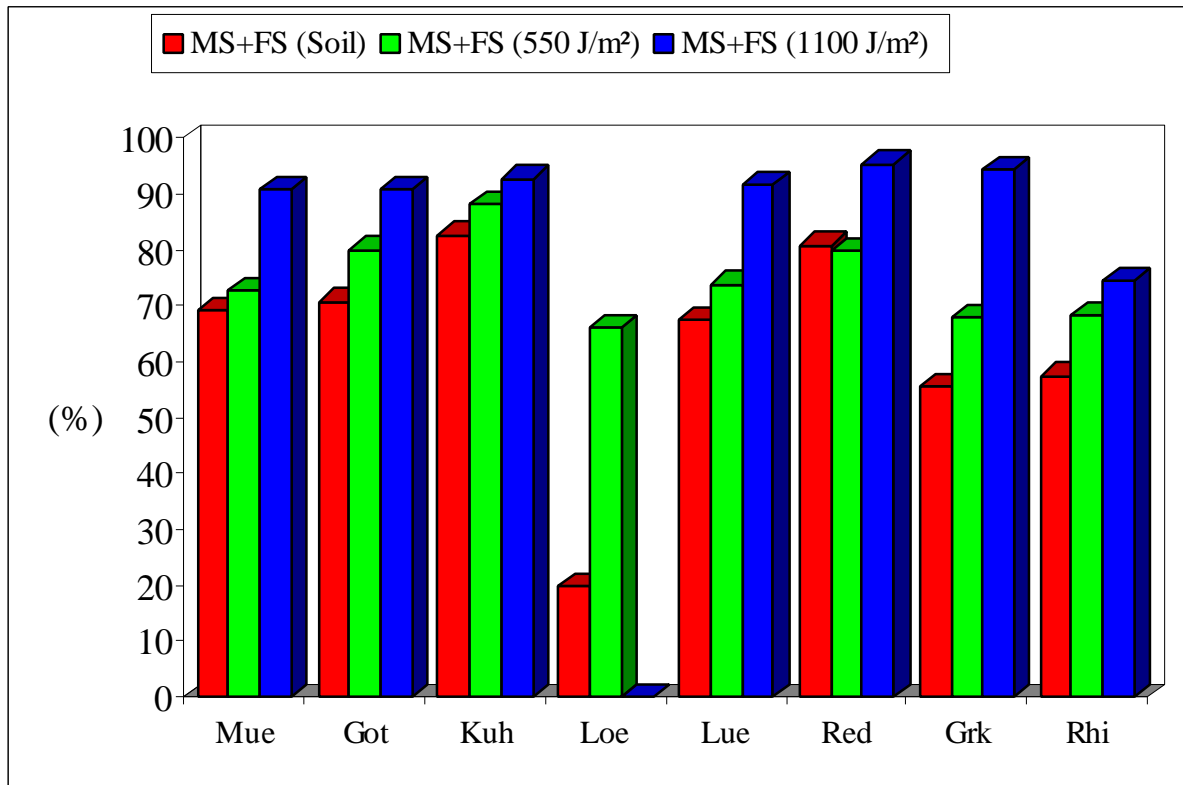


Figure 5: Comparison of the content of medium and fine sand (MS+FS) between the soils (red) and the LEM after rain of 550 J/m² (green) and 1100 J/m² (blue)

Crust stability

In the first step, the possible (maximum) shear force of the wind was calculated. The shear force can be calculated with $\tau = \rho u_*^2$ and reaches values smaller 1 Nm⁻² for a roughness only determined by the grains and a wind speed of 16 m/s in 0.5 m height.

There was no clear difference between the crust stability of the sandy soils after rainfall of 20 mm (or 550 J m⁻²). A crust could be measured only on the loamy soils (Figure 6). The crust breaking is only visible on the loess soil (Loe). The penetration pressure (force related to the cross section area) indicated the crust thickness very well (Figure 7), with 12 mm on the loess (Loe) and 5 mm on the loamy sand (Mue). The penetration pressure decreased with increased depth and values of all soils became more equal under the crusted layer independent of the soil type.

The comparison of the effects of all rainfall amounts on one soil is shown in Figure 8. The penetration force increased with increasing rain at a higher density of the surfaces. There is no sign for a crust (breaking) after 550 J/m². The maximum value is reached directly after the “touch down” of the cone. In the curve after rain of 1650 J/m² (60 mm) two steps indicate a crust breaking in 3 and 11 mm.

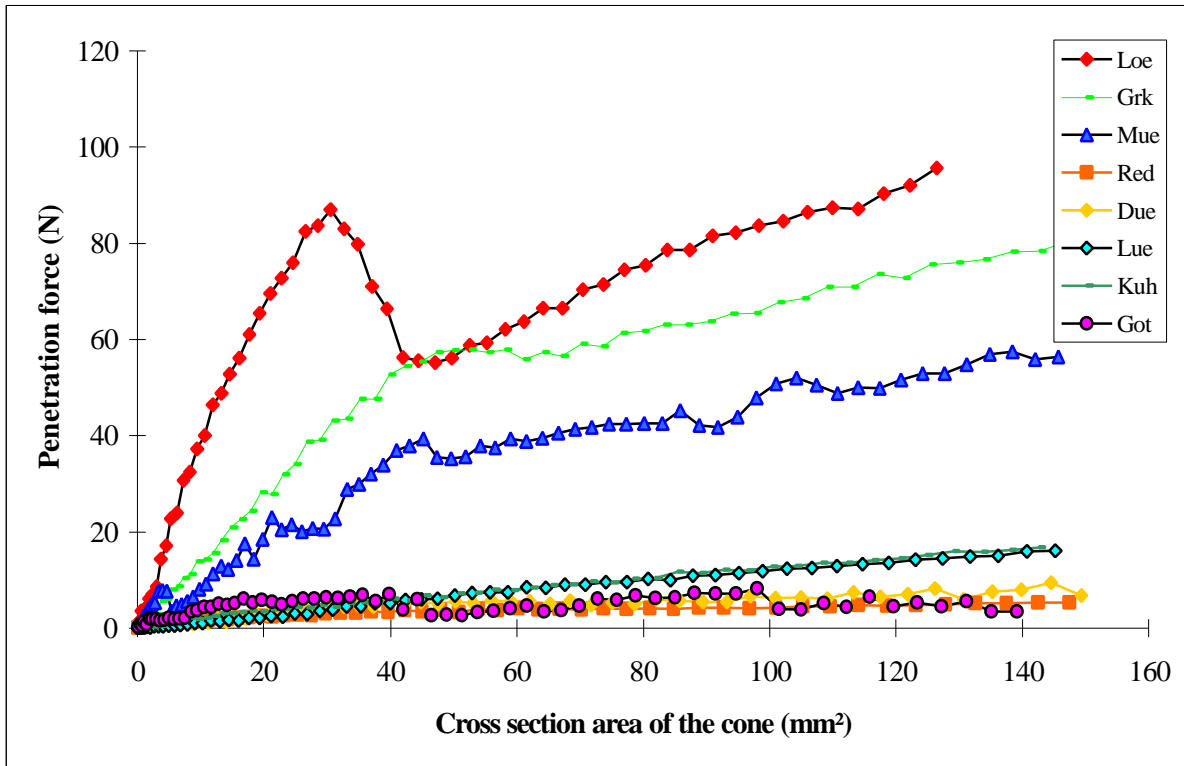


Figure 6: Penetration force (N) related to the cross section area of a cone after rainfall of 550 J/m² (20 mm)

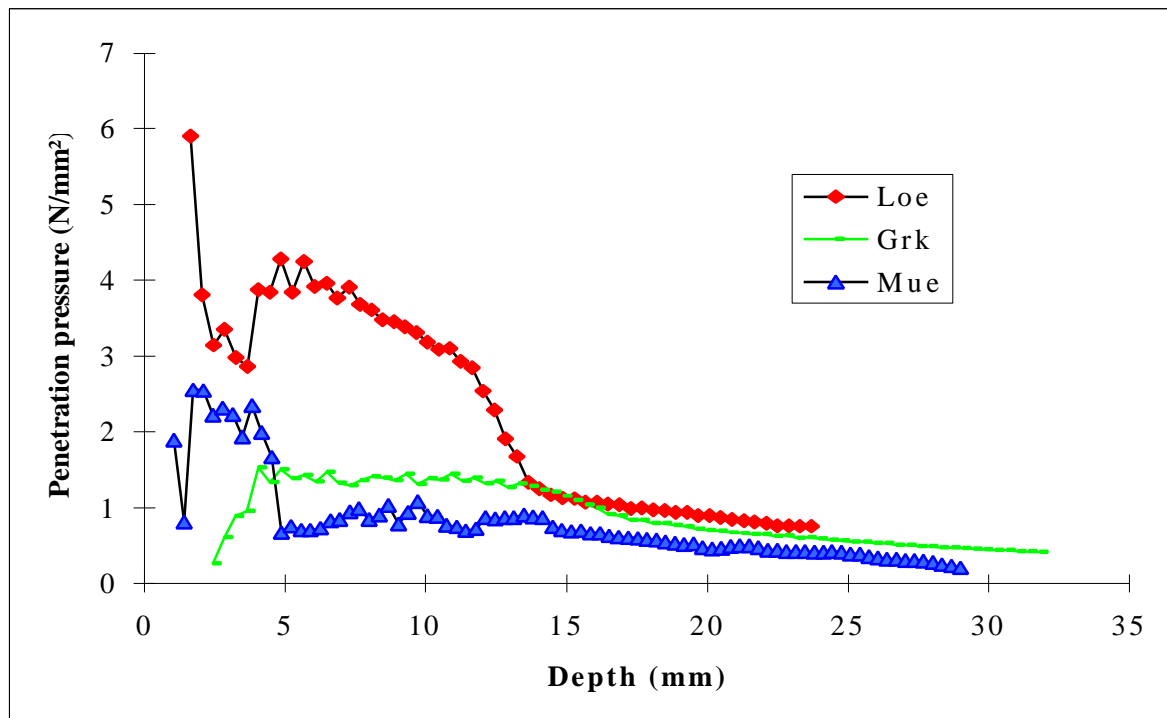


Figure 7: Penetration pressure related to the depth (only first three soils of Figure 6)

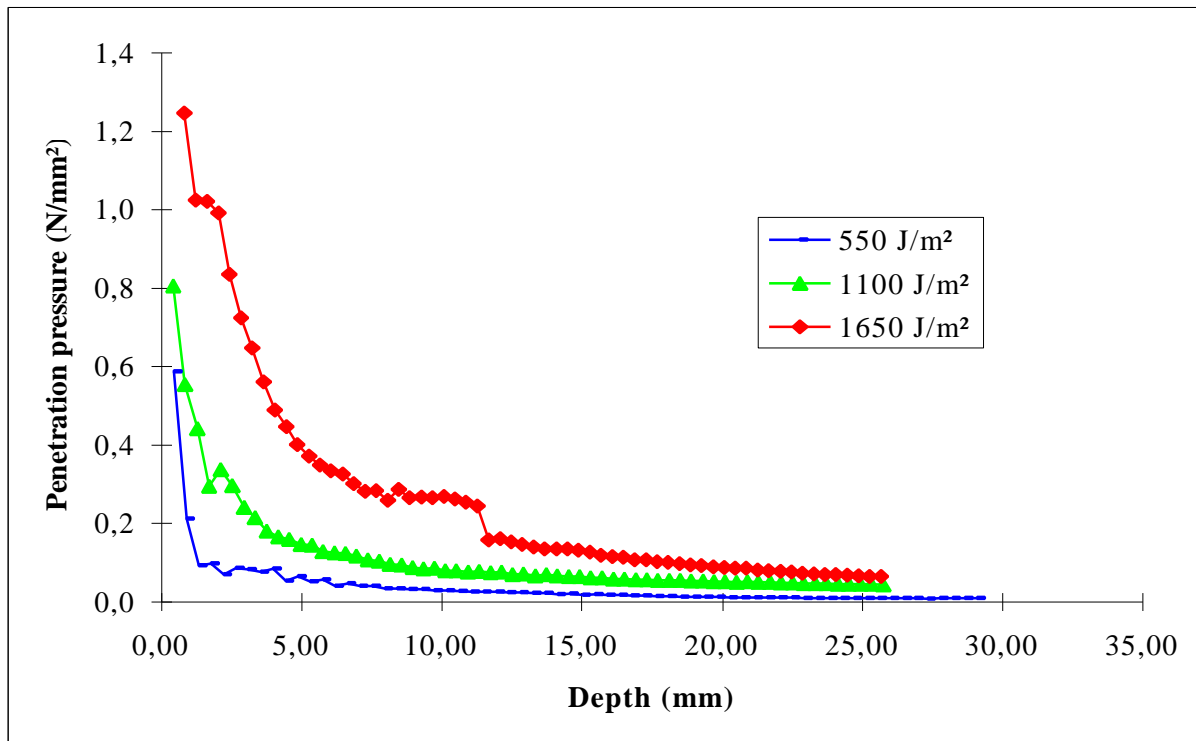


Figure 8: Penetration pressure related to the depth after rainfall with 550, 1100 and 1650 J/m² on a sandy soil (Red.)

Multiple regression was used to estimate the influence of soil parameters and the kinetic energy of the rainfall on the crust formation.

$$\begin{aligned}
 F_N &= 0.21 + 0.00005 E_{kin} - 0.002 (S\%) & r^2 &= 0.65*** \\
 F_N &= -0.0012 + 0.00005 E_{kin} + 0.003 (U\%) & r^2 &= 0.65*** \\
 F_N &= 0.016 + 0.00005 E_{kin} - 0.018 (T\%) & r^2 &= 0.63***
 \end{aligned}$$

The comparison of the measured forces of compression and the possible shear forces of the wind show that even weak crusts can resist the fluid impact. The difference related to the influenced surface is very large and amounts the factor to 10⁶. Therefore, other forces are necessary for the destruction of crusts, like the particle impact of saltating sand grains.

The application of penetration measurements only on crusts show encouraging results. Both the crust strength and the thickness can be estimated very exactly. The used rainfall simulator did not form a crust for rain of about 20 mm. The planned use of this method under field conditions will improve the results for a wider range of rainfall intensities.

Aggregate Stability

The kinetic stress of the aggregates was calculated from the wind speed and the feeding rate of the sand. Considering the scatter of the sand for each wind speed the following stresses were calculated (Table 4).

Table 4: Wind speed and kinetic stress of particle impact within abrasion experiments

u (m/s)	W_{kin} (N)	τ (N/m ²)
8	0.064	132
10	0.10	205
16	0.26	528

The kinetic energy of the particle impact increase by a factor greater than 100 in comparison with the pure fluid impact. Weak crusts can be abraded by these forces very fast. In Figure 9 the decrease of the volume of the aggregates depending on their sand content and the wind speed is shown. There are no significant results at a wind speed of 8 ms⁻¹ (near the threshold). Higher wind speed (or higher kinetic stress) results to an exponential decrease of the aggregate volume.

Regression analysis between the fractions and the shear force resulted in

$$\Delta V = -128 + 0.24 \tau + 1.4 S (\%) \quad r^2 = 0.53^{**}$$

$$\Delta V = 13.8 + 0.24 \tau - 1.68 U (\%) \quad r^2 = 0.54^{**}$$

$$\Delta V = 9.4 + 0.22 \tau - 5.7 T (\%) \quad r^2 = 0.4^*$$

The investigations have not been finished yet. The intention is the combination of the crust stability with the aggregate stability results to predict the crust resistance duration against abrasion.

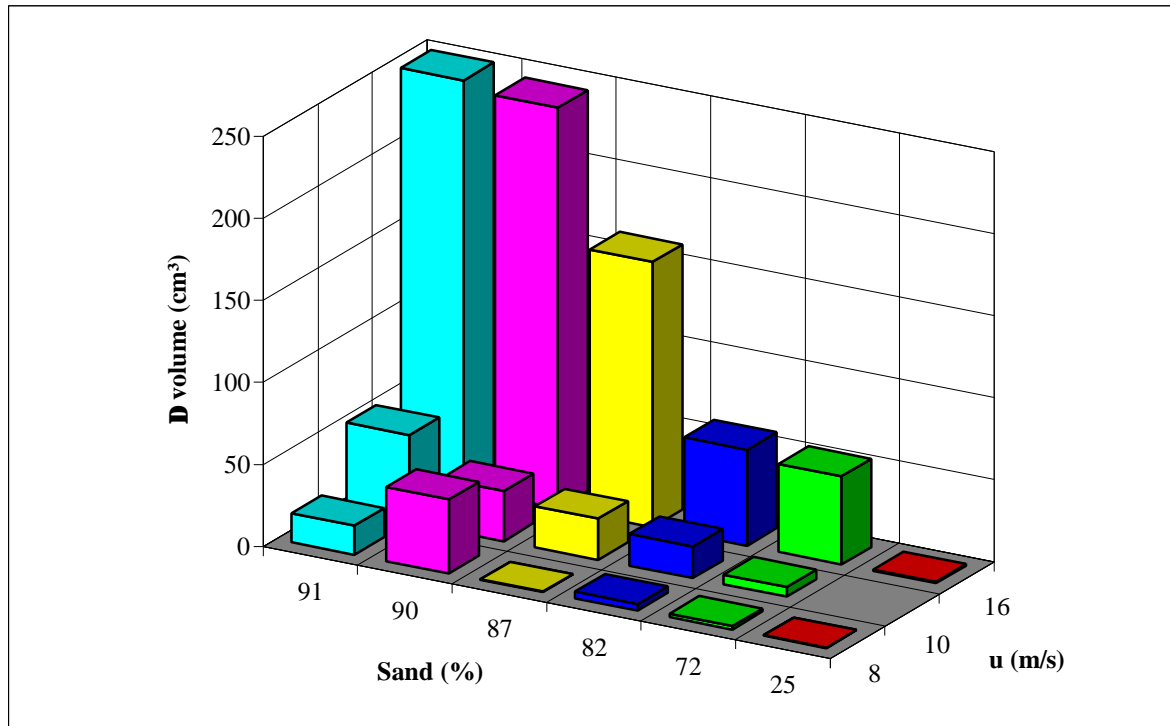


Figure 9: Decrease of the volume of aggregates depending on the sand content and the speed of abrading particles

Surface Drying

The difficulty to describe hydraulic functions results from their strong non-linearity. Therefore the priorities were set up to the gradient in water content on the soil surface and to a depth of 3 cm. Sandy soils show a homogeneous reaction: after constant decrease of water content to a critical point, the water content decreases rapidly and passes in very short time the threshold value for resistance against wind erosion (Figure 10). That shows that the surface water content can change from a not critical to a critical condition in very short times. The threshold was derived from field measurements where soil movement starts already from 3 % soil surface water content. The soil surface water content can decrease by 3 % within 1 mm PET.

The comparison between surface water content and the underlying water profile is shown in figure 11. Sandy soils have the greatest gradients. There are water contents of >15% at a depth of 3 cm, whereas the soil surface is dry and consequently susceptible to wind erosion. The work on this problem is in progress and further research is intended to come from the description of the process to a physical modeling.

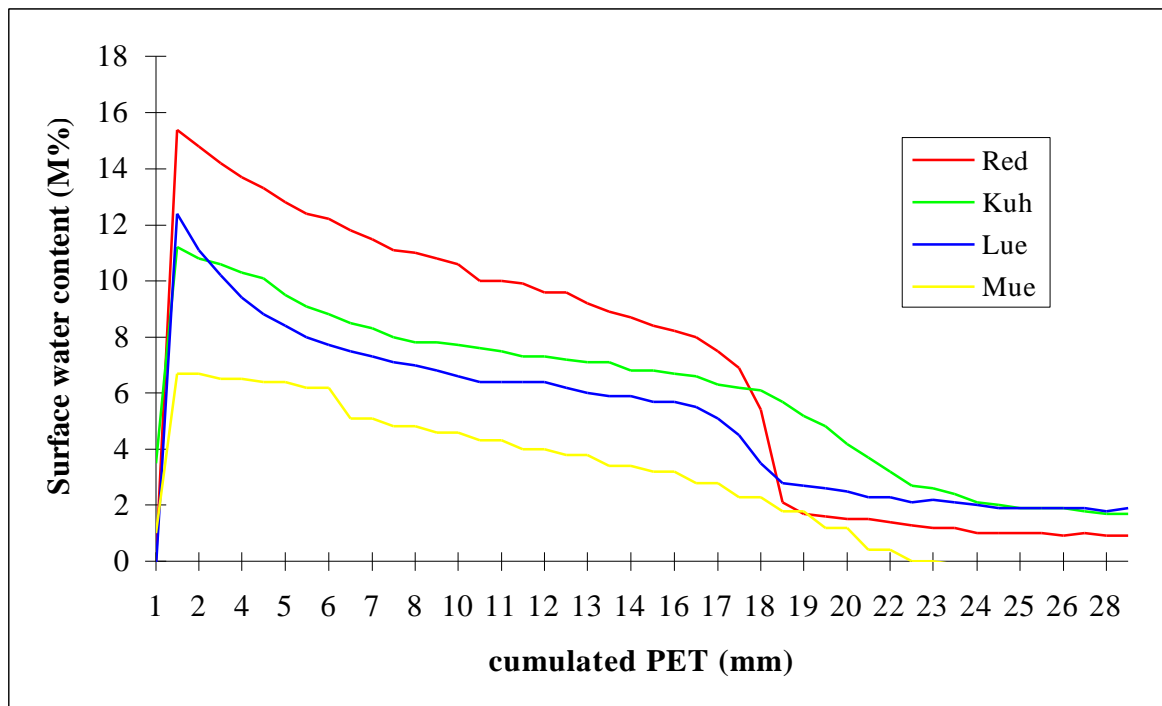


Figure 10: Surface water content in relation of the cumulated potential evapotranspiration

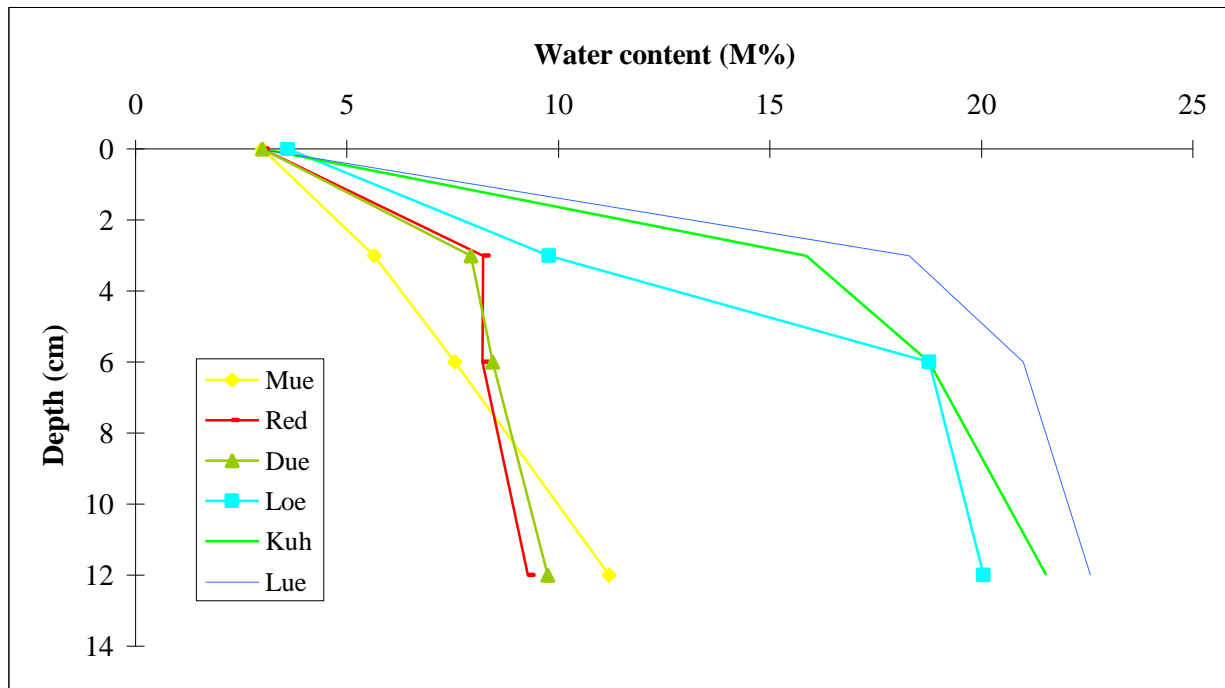


Figure 11: Water content gradients of soils by a surface moisture of 3%

Literature

- Chepil, W.S. (1951): Properties of soils which influence wind erosion: III. Effect of apparent density on erodibility. *Soil Sci.* 71, 141-153.
- FAO (1990): Guidelines for Soil Description. 3rd edition. FAO, Rome, 1990.
- Idso, S.B., R.D. Jackson, R.J. Reginato, B.A. Kimball & F.S. Nakayama (1975): The dependence of bare soil albedo on soil water content. *J. Appl. Meteorol.* 14, 109-113.
- Punzel, J. (1993): A proposed calculation of soil mechanical coefficients by penetrometer measurements (in German). *Archivs of Agronomy and Soil Science*, 37(6), 423-434.
- Reginato, R.J. (1975): Sampling soil-water distribution in the surface centimeter of a field soil. *Soil Sci.* 120(4), 292-294.
- Richter, J. (1986): *Der Boden als Reaktor. Modelle für Prozesse im Boden.* Ferdinand Enke Verlag Stuttgart.
- Roth, C. (1992): Die Bedeutung der Oberbodenverschlämmung für die Auslösung von Abfluss und Abtrag. *Bodenoekologie und Bodengeneese*, Bd. 6, 179 p.
- Valentin, C. (1992): Morphology, genesis and classification of surface crusts in loamy and sandy soils. *Geoderma*, 55: 225-245.
- Valentin, C., L.-M. Bresson (1992): Morphology, genesis and classification of surface crusts in loamy and sandy soils.- *Geoderma*, 55: 225-245.
- Wendling, U. H.-G. Schellin, M. Thomae (1991): Bereitstellung von taeglichen Informationen zum Wasserhaushalt des Bodens für die Zwecke der agrarmeteorologischen Beratung. *Z. Meteorol.* 41(6): 468-475.
- Zobeck, T. M. and W. M. Campbell (1990): Tillage and rainfall effects on near-surface density of sandy soils. ASAE-Paper 901080.
- Zobeck, T.M. and T.W. Popham (1992): Influence of microrelief, aggregate size and precipitation on soil crust properties. *Trans. ASAE* 35(2), 487-492.